


Synthesis and Structural Characterization of Four Different Concentrations of Ant Nest (*Myrmecodia pendens*) Collagen Membranes with Potential for Medical Applications

Dyah Nindita Carolina ^{1,2}, Mieke Hemiawati Satari^{3,*}, Bambang Pontjo Priosoeryanto^{4,*}, Agus Susanto^{1,*}, Cortino Sukotjo^{5,*}, Rahmana Emran Kartasasmita^{6,*}

¹Department of Periodontology, Dental Faculty, Universitas Padjadjaran, Bandung, West Java, Indonesia; ²Doctoral Study Program, Faculty of Medicine, Universitas Padjadjaran, Bandung, West Java, Indonesia; ³Department of Oral Biology, Dental Faculty, Universitas Padjadjaran, Bandung, West Java, Indonesia; ⁴Division of Veterinary Pathology, School of Veterinary Medicine & Biomedical Sciences, IPB University, Bogor, West Java, Indonesia; ⁵Department of Restorative Dentistry, College of Dentistry, University of Illinois at Chicago, Chicago, IL, 60612, USA; ⁶Research Group of Pharmaceutical Chemistry, School of Pharmacy, Institut Teknologi Bandung, Bandung, 40132, Indonesia

*These authors contributed equally to this work

Correspondence: Dyah Nindita Carolina, Department of Periodontology, Dental Faculty, Universitas Padjadjaran, Bandung, West Java, 40132, Indonesia, Tel +628156132636, Email dyah.nindita@unpad.ac.id

Purpose: The purpose of this study was to synthesize and structurally characterize four ant nest membranes in four different concentrations and determine the best concentration that could potentially be used as an alternative material for the production of new collagen barrier membranes.

Materials and Methods: Membranes were created by mixing ant nest extracts at various concentrations of 0.5%, 1%, 1.5%, and 2%, as well as collagen, chitosan, and Polyvinyl Alcohol (PVA) using a film casting. A Universal Testing Machine (UTM) was used to evaluate mechanical properties including elastic modulus, tensile strength, maximum elongation, elongation at break, and maximum force. Water absorption was performed, FTIR was used for functional group identification, and morphology was examined using SEM. Additionally, EDS was used to identify the composition and distribution of elements in membranes. Statistical analysis was conducted using ANOVA (analysis of variance) and post hoc testing with a significance level of $p < 0.01$ for quantitative data.

Results: The results showed that the mechanical properties produced the following mean (standard deviation): elastic modulus 0.87 Mpa (0.11), tensile strength 16.32 N/mm² (2.46), maximum elongation 4.96% (1.72), elongation at break 5.23% (1.87), and maximum force 22.50 N (5.06). The average water absorption capacity of all four membranes had a p -value < 0.01 . FTIR spectrum showed various peaks corresponding to functional groups, while SEM results indicated a homogeneous mixture. EDS analysis confirmed that the addition of ant plant extract at 0.5%, 1%, and 1.5% resulted in the presence of elements C, O, and Ca. Meanwhile, membranes prepared with 2% concentration had a different composition, namely C, O, Ca, and Na.

Conclusion: Increasing the concentration of ant nest affects the values of the membrane's mechanical properties parameters, including the elastic modulus (0.87 Mpa), tensile strength (16.32 N/mm²), maximum elongation (4.96%), elongation at break (5.23%), and maximum force (22.50 N). The average membrane absorption of water (p value < 0.01) was also affected. SEM images showed homogeneous mixing, and membrane EDS results consisted of C, O, and Ca composition. However, there was no effect on FTIR functional groups. The anthill membrane with a 1% concentration has the potential to serve as an alternative membrane in guided tissue regeneration.

Keywords: ant nest, carp scales, herbs, chitosan, polyvinyl alcohol, PVA

Introduction

Periodontal disease is a common oral health condition in Indonesia with a relatively high prevalence.¹ The 2018 National Basic Health Research (RISKESDAS) report showed that the highest incidence occurred in the age group of 35–44 years, ranging from 75.6% to 78.3%.² Furthermore, a study conducted by the National Institute of Dental and Craniofacial Research (NIDCR) in the United States stated that the prevalence was 90% in the adult population over 70 years.² These figures indicate that periodontal disease is relatively high in countries such as the United States and Indonesia.^{2,3}

The rise in periodontitis is primarily attributed to dental plaque bacteria as the main etiological factor. Periodontal pathogenic bacteria include *Aggregatibacter actinomycetemcomitans* (Aa), *Porphyromonas gingivalis* (Pg), and *Tannerella forsythia*. These bacteria release endotoxins that trigger the inflammatory process in periodontal tissues.¹ Inflammatory cells and exudate fluids cause degeneration of the connective tissue surrounding the gingiva, leading to clinical recession.² Damage to the collagen fibers at the apical portion of the junctional epithelium results in alveolar bone resorption. These clinical signs can lead to tooth mobility and loss.^{1,4,5}

The healing of bone tissue occurs in overlapping phases including inflammation, proliferation, and remodeling.⁶ The goal of remodeling is to achieve maximal bone healing regeneration,^{6,7} which can be achieved through reconstructive periodontal surgery.^{4,5} This procedure is usually performed in cases with severe tissue damage.^{8,9} This damage includes the alveolar bone and periodontal ligaments, often associated with more than two sides of the tissue. In many cases, there is vertical and angular bone damage, necessitating a matrix or material that can accelerate regeneration.^{8,9}

One of the potential natural sources of antioxidant compounds and natural preservatives is ant nest (*Myrmecodia pendens*). The genus *Myrmecodia* belongs to the *Rubiaceae* family, which is characterized as an epiphytic plant.¹⁰ The genus spreads from Malaysia, through the Philippines, Sumatra, Kalimantan, Java, Papua, New Guinea, Cape York to the Solomon Islands and the Pacific region.¹⁰ It has been empirically proven to treat gout, inflammation, muscle pain relief, immune strengthening, and cancer treatment. The largest species of *Myrmecodia* is found on the Indonesian islands of Papua and Papua New Guinea.¹⁰ Furthermore, the plant is considered epiphytic because it attaches to other plants but not as a parasite.¹¹ One effort to add value to wild ant plant is to investigate the chemical content analysis,^{10,11} including phytochemical and biological activity testing (such as antibacterial activity).¹²

Collagen has been shown to play a crucial role in clot formation and the hemostasis process. It attracts and activates fibroblast cells, promotes chemotaxis, has low immunogenicity, potentially increases tissue thickness, and interacts with various types of cells during wound healing.^{13–15} Several studies showed that fish scales affect wound healing¹⁶ due to the high collagen content. Fishery waste has diverse uses in the food industry, as well as to accelerate wound healing, and is a cost-effective raw material (waste) for pharmaceutical and cosmetic products. Furthermore, fish scales, skin, and bones are alternative sources for collagen production with great potential in dentistry. The collagen-based gel from tilapia fish scales exhibited anti-inflammatory activity in the healing process of incision wounds.^{16–18}

The use of collagen as barrier membranes in GBR (Guided Bone Regeneration) has been widely practiced. Membranes prepared using collagen-chitosan from white snapper scales affected wound healing, as evidenced by increased fibroblasts and new blood vessel formation.¹⁷

This study aimed to produce collagen membranes from carp fish (*Cyprinus carpio*) scales with the addition of ant plant extract. The physicochemical characteristics of the samples were also examined.

Materials and Methods

This study used an exploratory and descriptive method, with the aim to produce membranes using a composition of ant plant extract and collagen from carp scales. The ant nest (*Myrmecodia pendens*) based on Plant Identification Sheet: No.156/LBM/IT/II/2023 issued by Herbarium Jatinangor, Biosystematics and Molecular Laboratory, Department of Biology, Faculty of Mathematics and Natural Sciences Unpad. The name of the botanist who officially identified the anthill plant is Irwansyah Manurung, who has identified the plant with collection number was 178. The present study employed freshly obtained carp scales from collectors in Kajojo, Antapani-Bandung, Indonesia. Collagen membranes were previously produced with 3% fish scales, 2% chitosan, and 7.5% Polyvinyl Alcohol (PVA). In this study, ant plant extract was added at concentrations of 0.5%, 1%, 1.5%, and 2% (%w/v). The resulting membranes were subjected to

testing for physical properties including thickness, width, and length gauge, as well as mechanical properties, namely, elastic modulus, tensile strength, maximum elongation, elongation at break, and maximum force. Additionally, water absorption capacity, Fourier transform infrared (FTIR), Scanning Electron Microscopy (SEM), and Energy Dispersive X-ray Spectroscopy (EDS) tests were also conducted. This study was carried out at the School of Pharmacy Laboratory, Bandung Institute of Technology, and the Laboratory of PT Biomedical Technology Indonesia, a subsidiary of PT BLST Holding Company of Institut Pertanian Bogor.

Materials

The materials used for making collagen membranes included ant plant extract, carp scales collagen, 2% chitosan, and 7.5% PVA. The equipment used comprised a homogenizer mixer, petri dishes, plastic molds measuring 7.5 cm × 7.5 cm, glassware, and laboratory equipment. A Universal Testing Machine (UTM) Shimadzu AGS-X series 10 kN was used for the mechanical test, and SEM testing was conducted using a Thermofisher Quanta 650 instrument. EDS analysis was carried out with an Oxford Instruments 15 Xplore instrument, while FTIR analysis was performed using a Bruker Tensor 37 instrument with an MIR light source, DTGS detector, 4 cm⁻¹ instrument resolution, and 32 scans.

Preparation of Ant Nest Extract-Collagen-Chitosan-PVA Membranes

About 3% of collagen solution in acetic acid was prepared followed by overnight homogenization. Moreover, a 2% chitosan solution was made by mixing 4 g chitosan, 2 mL acetic acid, and 194 mL distilled water. The solution was then homogenized overnight followed by the preparation of a 7.5% PVA solution. The plant extract solutions with concentrations of 0.5%, 1%, 1.5%, and 2% were made using ethanol as the solvent. The prepared solutions of ant plant extract-collagen-chitosan-PVA were mixed in a 1:1:1:1 ratio, followed by overnight homogenization. The mixture was poured into acrylic molds measuring 7.5 × 7.5 cm with a weight of 10 g and allowed to dry at room temperature for a minimum of 3–4 days to achieve consistent results. The dry membranes were immersed in NaOH for 1 hour and washed until a neutral pH was achieved. Subsequently, membranes were frozen in a freezer at -80°C

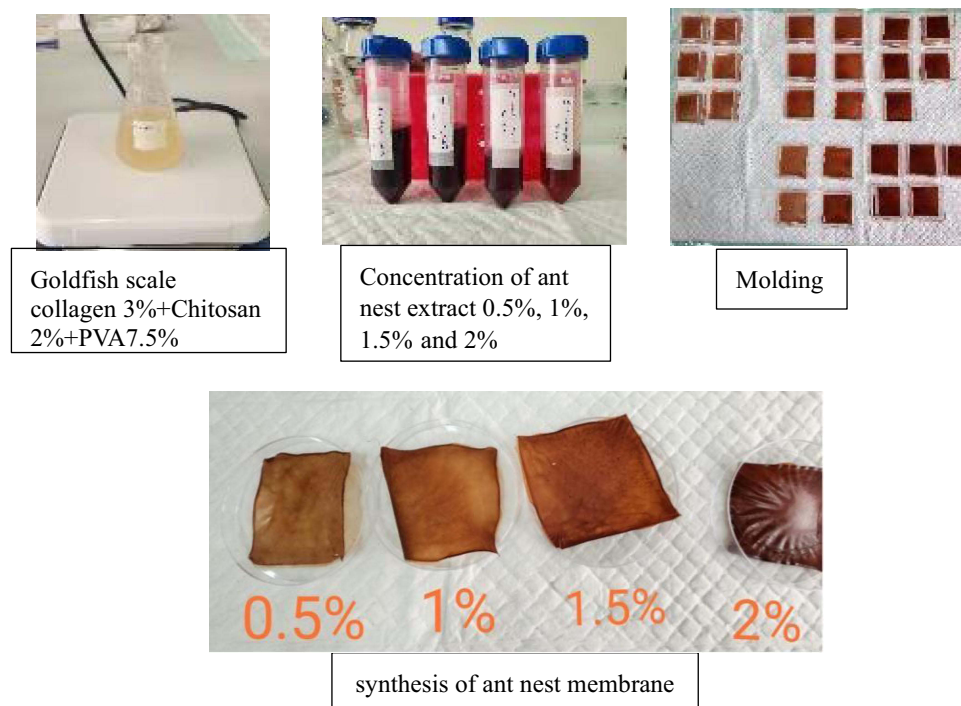


Figure 1 Preparation and synthesis of membranes with the addition of ant nest extract.

for 24 hours and dried using lyophilization or freeze-drying with a freeze dryer for 4 hours. The products were packaged in polypropylene plastic bags and irradiated using gamma rays at a radiation dose of 25 kGy. Four membranes with different compositions were prepared including plant extract of 0.5% (P1), 1% (P2), 1.5% (P3), and 2%-Collagen-Chitosan-PVA (P4).

Testing the Mechanical Properties of Membranes

The physical dimensions of composite membranes, including thickness, width, and gauge length, were measured. The mechanical properties were tested by measuring the elastic modulus, tensile strength, maximum elongation, elongation at break, and maximum force. The test procedures referred to the American Standard Mechanical method (ASTM D3039) using UTM Shimadzu AGS-X series 10 kN.¹⁹ Standard dumbbell-shaped membranes with two ends were clamped in the

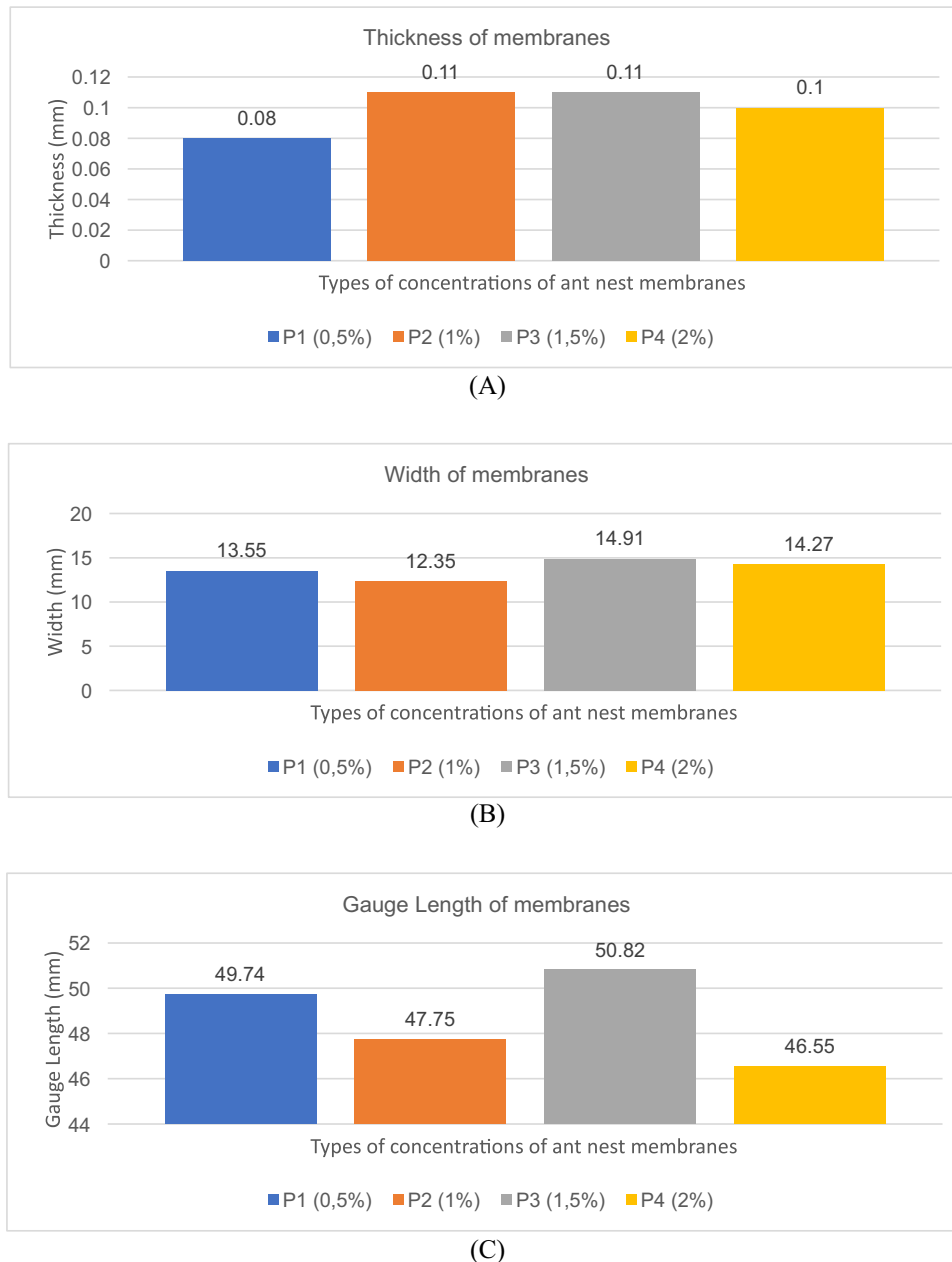


Figure 2 The thickness (A), width (B), and gauge length (C) of membranes added with ant plant extract (0.5%, 1%, 1.5%,2%) and Cyprinus carpio scale collagen 3%-Chitosan 2%-PVA 7.5%.

machine in an upper and lower position. Subsequently, one end of the membrane was pulled upward by the machine, and after the central part broke, the initial distance (L_0) and the break distance (L_1) were measured.¹⁹

$$\text{Elongation at break} = \frac{(L_1 - L_0)}{L_0} \times 100\%$$

Water Absorption Testing of Membranes

Composite membranes, both irradiated and non-irradiated, were cut into sizes of $1.5 \times 1 \text{ cm}^{20}$ and dried in an oven at 40°C for 24 hours until a constant weight (W_0) was reached. Subsequently, membranes were immersed in

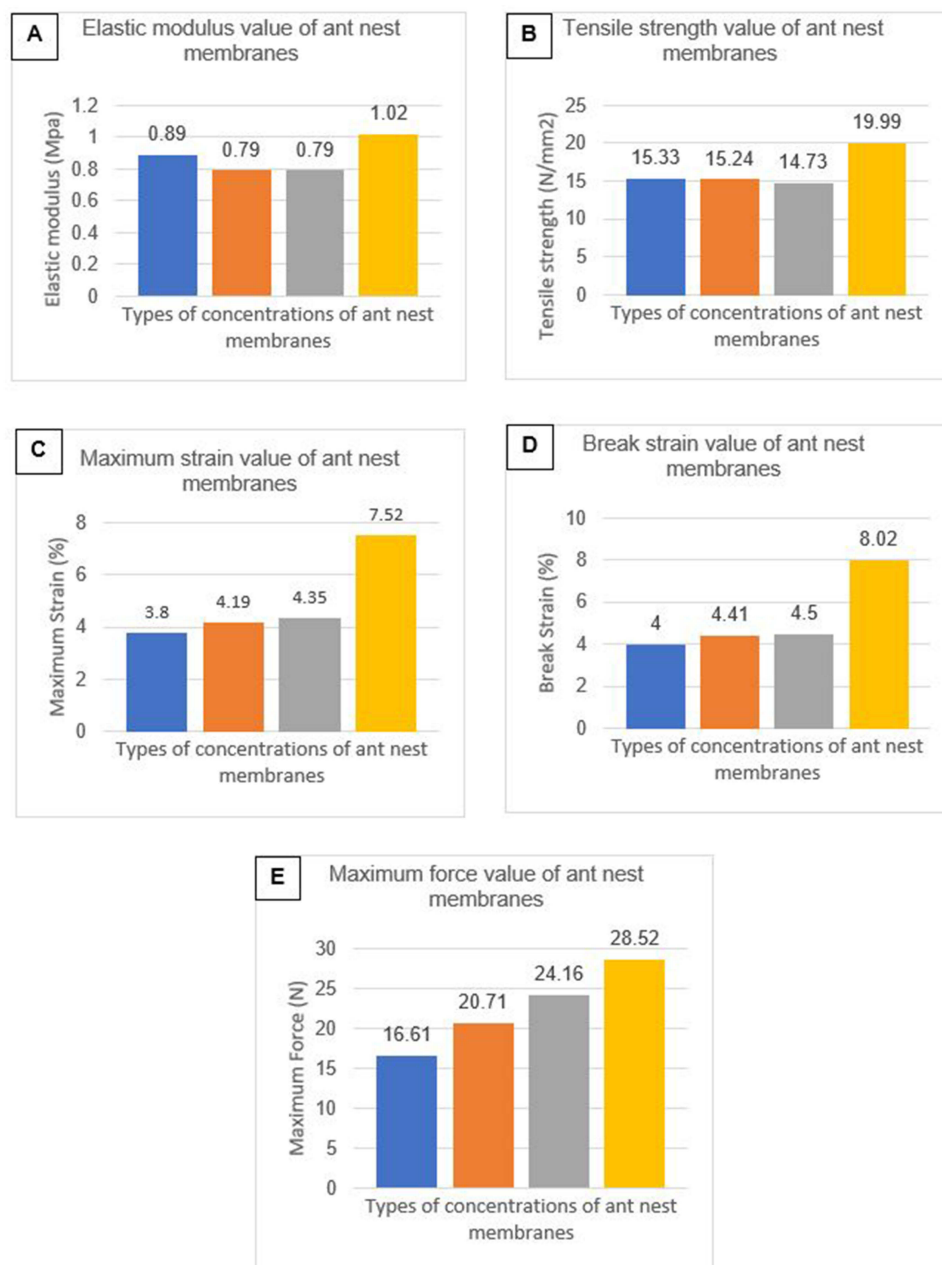


Figure 3 The elastic modulus value (A), tensile strength value (B), maximum strain value (C), break strain value (D), and maximum force value (E) of membranes added with ant plant extract (0.5%, 1%, 1.5%, 2%) and Cyprinus carpio scale collagen 3%-Chitosan 2%-PVA 7.5%.

distilled water with a volume of 50 mL for various durations of up to 24 hours to confirm complete swelling.²⁰ The samples were placed on filter paper to remove surface water followed by weighing (W1).^{20,21} The water absorption was calculated using the equation:²¹

$$\text{Water Absorption} = \frac{W1 - W0}{W0} \times 100\%$$

Analysis of Functional Groups Using FTIR Spectrophotometer

Ant plant composite membranes were cut into small pieces (0.2 × 0.2 mm), placed on KBr powder, and then analyzed using an FTIR spectrophotometer in the wave number range of 4000 cm⁻¹ to 500 cm⁻¹.^{22,23}

Morphology Testing (SEM)

Morphological testing and analysis were conducted using SEM.²⁴

Elemental Composition Testing (EDS)

EDS was used to identify the composition and distribution of elements in membranes,²⁴ after completing SEM observations.^{24,25}

Statistical Analysis

Data were presented descriptively including the mean values and standard deviations of the triple measurements, as well as ANOVA (analysis of variance) with a significance level of $p < 0.01$ for the water absorption testing results. Physical and mechanical test results were presented in tabular form. Qualitative analysis was conducted using FTIR spectrophotometer by comparing the similarity of spectra based on the match factor (MF) parameter. The results of SEM evaluation were also described qualitatively, and tables of EDS test results were presented.

Results

Figure 1 shows the preparation and synthesis of membranes with the addition of ant nest extract. The dimensions of the four membranes with different concentrations of ant plant extract are shown in Figure 2. The thickness values obtained included P1: 0.08 mm, P2: 0.11 mm, P3: 0.11 mm, and P4: 0.1 mm, while the width was as follows: P1 (13.55 mm), P2 (12.35 mm), P3 (14.91 mm), and P4 (14.27 mm). Additionally, the values for the gauge length were P1: 49.74 mm, P2: 47.75 mm, P3: 50.82 mm, and P4: 46.55 mm.

Tensile strength and elongation at break represent the maximum stress a material can withstand when pulled before breaking. The results for the modulus of elasticity, tensile strength, maximum elongation, elongation at break, and maximum force are presented in Figure 3. UTM results showed that the mean and standard deviations were as follows: 0.87 Mpa (0.11), 16.32 N/mm² (2.46), 4.96% (1.72), 5.23% (1.87), and 22.50 N (5.06), respectively.

Table 1 Absorption Capacity of Ant Plant Membranes

Ant Plant Membranes	Average ± SD
P1	433.331±5.45*
P2	668.042±0.32*
P3	217.813±0.37*
P4	197.014±0.53*

Notes: P1: Membranes with 0.5% ant plant extract, P2: 1% ant plant extract, P3: 1.5% ant plant extract, P4: 2% ant plant extract. Significance value $P = * = p < 0.001$.

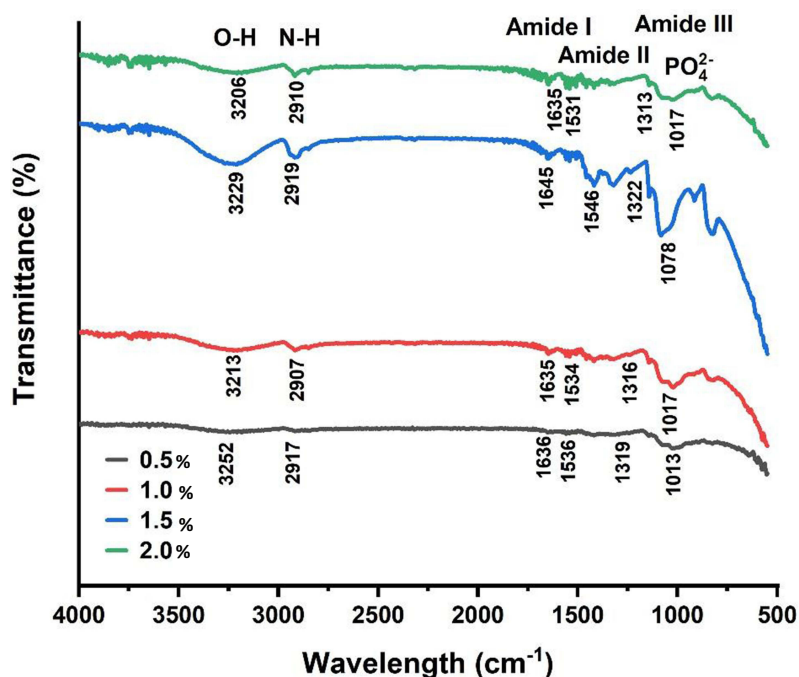


Figure 4 FTIR spectrum of ant plant membranes 0.5% (grey line), 1% (red line), 1.5% (blue line) and 2% (green line).

The results of the water absorption measurements conducted three times on membranes with concentrations of 0.5%, 1%, 1.5%, and 2% are shown in Table 1. ANOVA showed $p < 0.001$, indicating a highly significant difference between treatments.

FTIR results are presented in Figure 4, while the characteristics of functional groups in ant plant membranes are shown in Table 2.

In the amide A absorption curve, samples P1, P2, P3, and P4 showed a broad absorption at $3252\text{--}2917\text{ cm}^{-1}$, $3213\text{--}2907\text{ cm}^{-1}$, $3229\text{--}2919\text{ cm}^{-1}$, and $3206\text{--}2910\text{ cm}^{-1}$, while for amide I, broad absorptions were observed at 1636 cm^{-1} , 1635 cm^{-1} , 1645 cm^{-1} , and 1635 cm^{-1} , respectively. The amide II absorption regions for samples P1, P2, P3, and P4 were at 1536 cm^{-1} , 1534 cm^{-1} , 1546 cm^{-1} , and 1531 cm^{-1} . The last specific absorption region was amide III, at 1319 cm^{-1} , 1316 cm^{-1} , 1322 cm^{-1} , and 1313 cm^{-1} , respectively. FTIR test results also detected the spectrum curve of PO_4^{2-} in all four samples.

The SEM test results were presented in Figure 5 and the surface pores in (A) showed that the addition of 0.5% ant plant extract resulted in the largest pores and the most widely spaced fiber bonds. This was followed by smaller pore sizes in (Figure 5B and C) with the addition of 1% and 1.5% concentrations, respectively. The 2% ant plant extract

Table 2 FTIR Functional Groups of Ant Plant Membranes

Functional Group	Wavelength (cm-1)	Wavelength (cm-1)			
		P1	P2	P3	P4
O-H stretching	3750–3000	3252	3213	3229	3206
N-H stretching	3300–3500	2917	2907	2919	2910
Amide I	1600–1690	1636	1635	1645	1635
Amide II	1480–1575	1536	1534	1546	1531
Amide III	1229–1301	1319	1316	1322	1313
PO_4^{2-}		1013	1017	1078	1017

Notes: P1: Membranes with 0.5% ant plant extract, P2: 1% ant plant extract, P3: 1.5% ant plant extract, P4: 2% ant plant extract.

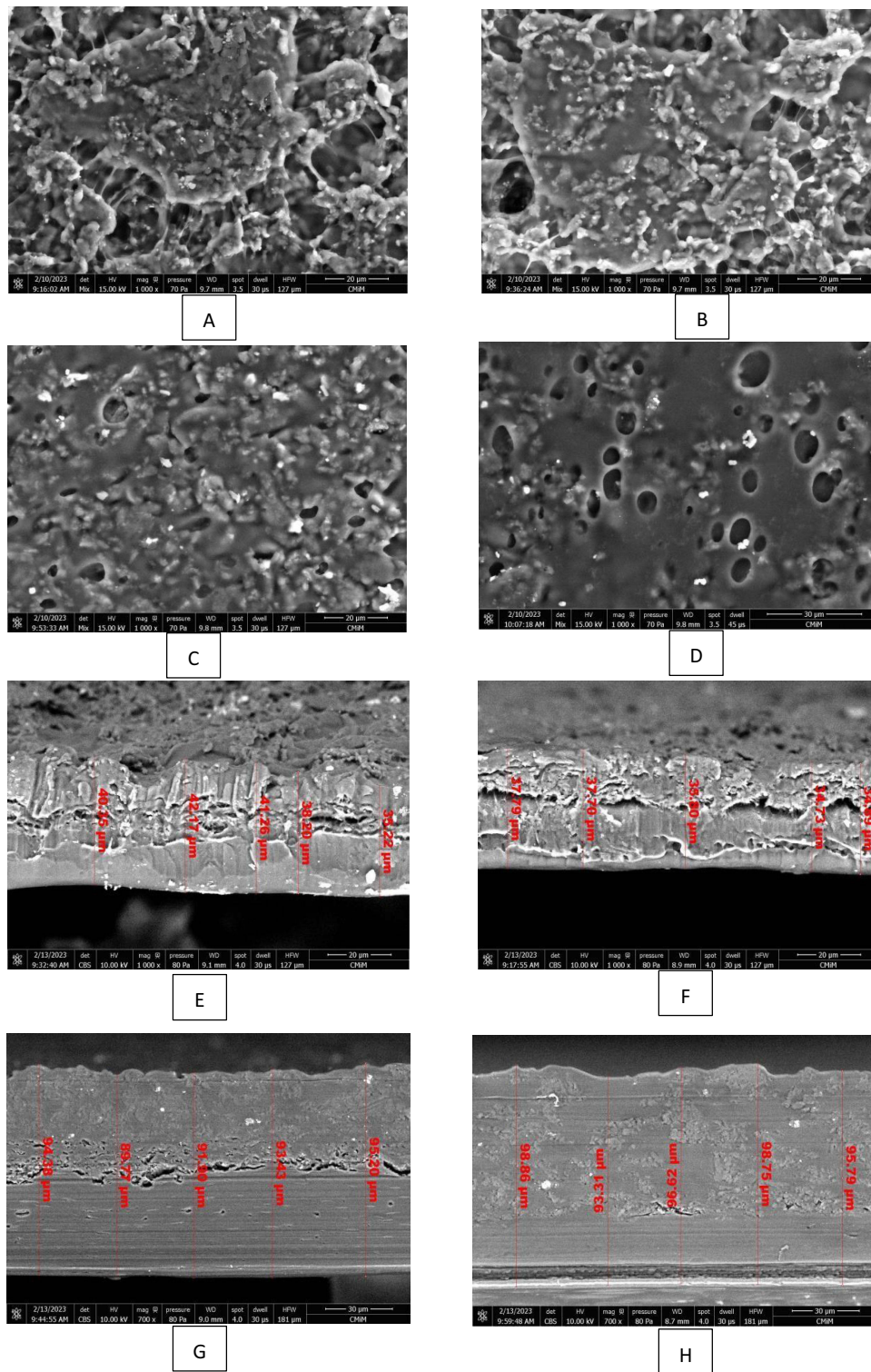


Figure 5 SEM results with a 1000x (scale 20 µm) magnification of collagen membranes from carp scales with the addition of ant plant extract (A) 0.5%, (B) 1%, (C) 1.5%, and (D) 2%. SEM cross-section results with a 1000x magnification of collagen membranes from carp scales with the addition of ant plant extract (E) 0.5%, (F) 1%, (G) 1.5%, and (H) 2%.

concentration in (Figure 5D) yielded the smallest pores and the closest fiber bonds, but air bubbles remain present. The sizes of membranes cross-section were as follows: (Figure 5E) 35.22 to 40.35 µm, (Figure 5F) 34.73 to 37.79 µm, (Figure 5G) 89.77 to 95.20 µm, and (Figure 5H) 93.31 to 98.86 µm.

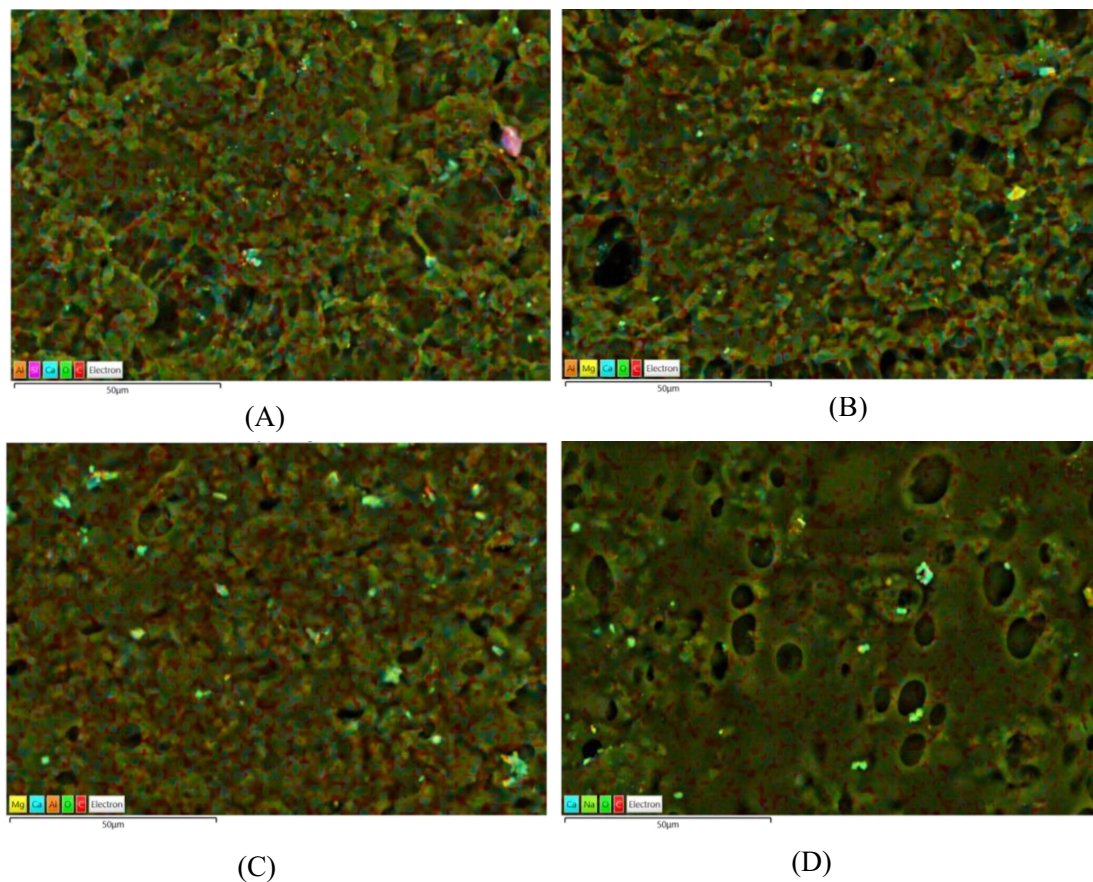


Figure 6 EDS spectrum results with a 1000x (scale 20 µm) magnification of collagen membranes from carp scales with the addition of ant plant extract (A) 0.5%, (B) 1%, (C) 1.5%, and (D) 2%.

The spectra for the distribution of elements or components of membranes based on the EDS test are shown in Figure 6 and Table 3. P1 consisted of C (56.2%), O (42.6%) and Ca (0.7%), P2: C (58.2%), O (40.7%) and Ca (0.8%), P3: C (59.1%), O (39.6%) and Ca (0.5%), as well as P4: C (60.1%), O (39.2%), Ca (0.3%) and Na (0.4%).

Discussion

Based on the results, the thickness of membranes did not significantly affect mechanical properties. The tested membranes had a smaller thickness (0.20 mm) and a higher maximum tensile stress (13.0 MPa) than Bio-gide[®], Remaix[®], and OssixPlus[®].^{26,27} The differences in the properties may be attributed to variations in materials and microstructure. The samples studied had a maximum tensile strength of 14.43 MPa, well above Bio-gide[®] and other

Table 3 EDS Result of Ant Plant Membranes

Ant Plant Membranes	Elements (%)			
	C	O	Ca	Na
P1	56.2	42.6	0.7	–
P2	58.2	40.7	0.8	–
P3	59.1	39.6	0.5	–
P4	60.1	39.2	0.3	0.4

Notes: P1: ant plant 0.5%, P2: ant plant 1%, P3: ant plant 1.5%, P4: ant plant 2%.

commercial products, indicating better clinical performance.²⁷ The results in Figures 1 and 2 showed that the addition of different ant plant concentrations significantly affected gauge thickness, width, and length. The treatment also caused variations in the values of elastic modulus, tensile strength at break, maximum elongation, elongation at break, and maximum force.

The ability to absorb water is one of the parameters in membrane characterization. Based on the results, the highest absorption was observed in membranes with the lowest chitosan/collagen mixture.²⁸ Table 1 presents unique variations in absorption capacity, where the sample added with 1% concentration had the highest absorption capacity compared to others.

The SEM results in Figure 3 shows that the higher the concentration of ant plant extract added, the smaller the visible pore image. However, air bubbles were present in the sample prepared by adding 2% ant extract. Membranes exhibited a microarchitecture of pores and interconnections in their surface, providing space for vascularization.²⁹ The main limitation of electron microscopy is the fixation and dehydration procedures during biological tissue preparation. These challenges are further exacerbated by the use of NaOH in tissue processing.³⁰ To mitigate these limitations, electron microscopy can be enhanced by second wave generation (SHG) and two-photon induced fluorescence (TPEF), which provide a comprehensive view of the fiber arrangement across membranes.³⁰

EDS microanalysis is an elemental analysis technique commonly used in conjunction with electron microscopy to identify the presence of elements in a sample.³¹ Figure 4 and Table 3 show that the four membranes contain the C element as a marker for the presence of organic components.

Conclusion

In conclusion, ant plant membranes have the potential to be developed for guided tissue regeneration. Based on the results, increasing the concentration of the extract affected the mechanical properties (elastic modulus (0.87 Mpa), tensile strength (16.32 N/mm²), maximum elongation (4.96%), elongation at break (5.23%), and maximum force (22.50 N)), as well as water absorption (p value <0.01), SEM images showing homogeneous mixing, and EDS parameters consisting of C, O, and Ca composition. However, the FTIR results showed that there was no change in the absorption peaks in all treatments, indicating no change in the functional groups. The anthill membrane with 1% concentration has the potential to be used as an alternative membrane in guided tissue regeneration.

Acknowledgments

We are thankful to Kemendikbud Dikti for the research fund.

Funding

This study was supported by the BPPDN Domestic Postgraduate Education Scholarship from the Ministry of Education, Culture and Research, Technology of Indonesia (Kemendikbud Dikti) in 2019.

Disclosure

The authors report no conflicts of interest in this work.

References

1. Hinrichs JE, Novak MJ. Classification of diseases and conditions affecting the periodontium. In: Newman MG, Takei HH, Carranza FA, editors. *Carranza's Clinical Periodontology*. 11th ed. St. Missouri: Elsevier Saunders; 2012:41–42.
2. Philstrom B, Michalowicz B, Johnson N. Periodontal Diseases. *Lancet*. 2005;366:1809. doi:10.1016/S0140-6736(05)67728-8
3. Riset Kesehatan Dasar (Riskesdas) 2018. Available from: <https://repository.badankebijakan.kemkes.go.id/id/eprint/3514/>. Accessed May 17, 2024.
4. Carranza FA, Camargo PM. The Periodontal Pocket. Dalam. In: Newman MG, Takei HH, Carranza FA, editors. *Carranza's Clinical Periodontology*. 11th ed. St. Missouri: Elsevier Saunders; 2012:127–139.
5. Agnihotram G, Singh TRM, Pamidimarri G, Jacob L, Rani S. Study of clinical parameters in chronic periodontitis. *Int J Appl Biol Pharmaceut Technol*. 2010;1(3):1202–1208.
6. Andrade I, Taddei RAS, Souza EAP. Inflammation and tooth movement: the role of cytokines, chemokines, and growth factors. *Semin Orthodont*. 2012;18:257–269. doi:10.1053/j.sodo.2012.06.004

7. Walgenbach KJ, Voight M, Riabikhin AW, Andree C, Schaefer DJ, Galla TJ. Tissue engineering in plastic reconstructive surgery. *Anat Rec.* 2001;263(4):372–378. doi:10.1002/ar.1117
8. Takei HH, Nevin ML, Cochran DL, Carranza FA, Reynold MA. Reconstructive periodontal surgery. In: Newman MG, Takei H, Klokkevold C, editors. *Carranza's Clinical Periodontology*. 11th ed. St. Missouri: Elsevier Saunders; 2012:577–588.
9. Richard T, Nishimine D, Dault S. Tissue engineering for periodontal regeneration. *Journal CDA.* 2005;33(3):205–215.
10. Dirgantara S, Insanu M, Fidrianny I. Medicinal Properties of Ant Nest Plant (Myrmecodia Genus): a comprehensive review. *Open Access Maced J Med Sci.* 2022;10(F):97–103. doi:10.3889/oamjms.2022.8481
11. Sudiono J, Hardina M. The effect of Myrmecodia pendans ethanol extract on inflamed pulp: study on Sprague Dawley rats. *Mol Cell Biomed Sci.* 2019;3(2):115–121. doi:10.21705/mcbs.v3i2.70
12. Parin FN, El-Ghazali S, Yeşilyurt A, et al. PVA/inulin-based sustainable films reinforced with pickering emulsion of niaouli essential oil for potential wound healing applications. *Polymers.* 2023;15(4):1002. doi:10.3390/polym15041002
13. Einhorn Thomas A. "Orthopaedic Basic Science Fundamental of Clinical Practice". 3th Vol. P. Americans Orthopaedic Association; 2012.181–188.
14. Burkitt GH, Young B, Heath JW. *Wheater's Functional Histology*. 3rd ed. Melbourne: Churchill Livingstone; 2003:180:176–7.
15. Abbas AK, Lichtman AH, Poher JS. Cytokines. In: Abbas AK, editor. *Cellular and Molecular Immunology*. 5th ed. Philadelphia: WB Saunders company; 2011:235–242.
16. Ang J, Pierezan F, Kim S, et al. Use of topical treatments and effects of water temperature on wound healing in common carp (*Cyprinus carpio*). *J Zoo Wildl Med.* 2021;52(1):103–116. doi:10.1638/2020-0072
17. Susanto A, Susana S, Pontjo Priosoeryanto B, Hemiawati Satari M, Komara I. The effect of the chitosan-collagen membrane on wound healing process in rat mandibular defect. *J Indian Society.* 2019;23(2):113–118.
18. Komara I, Susanto A, Amaliya A, et al. The effect of gamma-ray irradiation on the physical, mechanical, and morphological characteristics of PVA-collagen-chitosan as a guided tissue regeneration (GTR) membrane material. *Eur J Dent.* 2023;17(2):530–538. doi:10.1055/s-0042-1753451
19. ASTM Committee D-30 on Composite Materials. Standard test method for tensile properties of polymer matrix composite materials. *ASTM Int.* 2008;2008:1.
20. Hestiawan H. The water absorption, mechanical and thermal properties of chemically treated woven fan palm reinforced polyester composites. *J Mater Res Technol.* 2020;9(3):4410–4420. doi:10.1016/j.jmrt.2020.02.065
21. Bajpai M, Bajpai SK, Jyotishi P. Water absorption and moisture permeation properties of chitosan/poly (acrylamide-co-itaconic acid) IPC films. *IJBM.* 2016;2016:1–9.
22. Raj SS, Kuzmin AM, Subramanian K, Sathiamoorthy S, Kandasamy KT. Philosophy of selecting ASTM standards for mechanical characterization of polymers and polymer composites. *Materiale Plastice.* 2021;58(3):247–256. doi:10.37358/MP.21.3.5523
23. Derkach SR, Kolotova DS, Kuchina YA, Shumskaya NV. Characterization of fish gelatin obtained from Atlantic cod skin using enzymatic treatment. *Polymers.* 2022;14(4):751. doi:10.3390/polym14040751
24. Kharin AY. Deep learning for scanning electron microscopy: synthetic data for the nanoparticle detection. *Ultramicroscopy.* 2020;219:113125. doi:10.1016/j.ultramic.2020.113125
25. Kurpaska L, Jozwik I, Jagielski J. Study of sub-oxide phases at the metal-oxide interface in oxidized pure zirconium and Zr-1.0% Nb alloy by using SEM/FIB/EBS and EDS techniques. *J Nucl Mater.* 2016;476:56–62. doi:10.1016/j.jnucmat.2016.04.038
26. Kopp J, Bonnet M, Renou J. Effect of collagen crosslinking on collagen-water interactions (A DSC Investigation). *Matrix.* 1990;9:443–450. doi:10.1016/S0934-8832(11)80013-2
27. da Silva Brum I, Elias CN, Nascimento ALR, de Andrade CBV, de Biasi RS, de Carvalho JJ. Ultrastructural and physicochemical characterization of a non-crosslinked type 1 bovine derived collagen membrane. *Polymers.* 2021;13(23):4135. doi:10.3390/polym13234135
28. Lukitowati F, Indrani D. Water absorption of chitosan, collagen and chitosan/collagen blend membranes exposed to gamma-ray irradiation. *Iran J Pharm Sci.* 2018;14(1):57–66. doi:10.22034/ijps.2018.32049
29. Susanto A, Satari MH, Abbas B, Koesoemowidodo RSA, Cahyanto A. Fabrication and characterization of chitosan-collagen membrane from barramundi (lates calcarifer) scales for guided tissue regeneration. *Eur J Dent.* 2019;13(3):370–375. doi:10.1055/s-0039-1698610
30. Maurer T, Stoffel MH, Belyaev Y, et al. Structural characterization of four different naturally occurring porcine collagen membranes suitable for medical applications. *PLoS One.* 2018;13(10):e0205027. doi:10.1371/journal.pone.0205027
31. Mulyawan I, Danuningrat CP, Soesilawati P, et al. The characteristics of demineralized dentin material sponge as guided bone regeneration based on the FTIR and SEM-EDX tests. *Eur J Dent.* 2022;16(4):880–885. doi:10.1055/s-0042-1743147

Clinical, Cosmetic and Investigational Dentistry

Dovepress

Publish your work in this journal

Clinical, Cosmetic and Investigational Dentistry is an international, peer-reviewed, open access, online journal focusing on the latest clinical and experimental research in dentistry with specific emphasis on cosmetic interventions. Innovative developments in dental materials, techniques and devices that improve outcomes and patient satisfaction and preference will be highlighted. The manuscript management system is completely online and includes a very quick and fair peer-review system, which is all easy to use. Visit <http://www.dovepress.com/testimonials.php> to read real quotes from published authors.

Submit your manuscript here: <https://www.dovepress.com/clinical-cosmetic-and-investigational-dentistry-journal>